Cell, Vol. 91, 109–118, October 3, 1997, Copyright ©1997 by Cell Press

The AP-3 Adaptor Complex Is Essential for Cargo-Selective Transport to the Yeast Vacuole

Christopher R. Cowles,*‡ Greg Odorizzi,*‡ Gregory S. Payne,† and Scott D. Emr*§

*Division of Cellular and Molecular Medicine
and Howard Hughes Medical Institute
University of California, San Diego
School of Medicine
La Jolla, California 92093-0668

†Molecular Biology Institute
and Department of Biological Chemistry
School of Medicine
University of California
Los Angeles, California 90024

Summary

Three distinct adaptor protein (AP) complexes involved in protein trafficking have been identified. AP-1 and AP-2 mediate protein sorting at the *trans*-Golgi network and plasma membrane, respectively, whereas the function of AP-3 has not been defined. A screen for factors specifically involved in transport of alkaline phosphatase (ALP) from the Golgi to the vacuole/lysosome has identified Apl6p and Apl5p of the yeast AP-3 complex. Deletion of each of the four AP-3 subunits results in selective mislocalization of ALP and the vacuolar t-SNARE, Vam3p (but not CPS and CPY), while deletion of AP-1 and AP-2 subunits has no effect on vacuolar protein delivery. This study, therefore, provides evidence that the AP-3 complex functions in cargo-selective protein transport from the Golgi to the vacuole/lysosome.

Introduction

In eukaryotic cells, transport of newly synthesized proteins through the secretory and endocytic pathways is mediated by membrane vesicles. The formation and budding of transport vesicles involves recruitment of cytosolic coat proteins to the donor membrane. In addition to providing the structural components necessary to drive vesicle budding, coat protein complexes impart cargo specificity by recognizing and packaging signal-bearing membrane proteins into the emerging vesicle (Schekman and Orci, 1996). Two types of clathrin-coated vesicles deliver cargo to the endocytic pathway by assembling on distinct compartments through interactions with different heterotetrameric adaptor protein (AP) complexes (Robinson, 1994). Clathrin-coated vesicles that bud from the *trans*-Golgi network (TGN) interact with AP-1, whereas those that bud from the plasma membrane interact with AP-2. The AP complexes not only provide a membrane-binding site for clathrin but also interact with trafficking membrane proteins to serve a cargo-selective function (Marks et al., 1997; Robinson, 1997).

‡The first two authors contributed equally to this work.
§To whom correspondence should be addressed.

In Saccharomyces cerevisiae, proteins homologous to the AP-1 and AP-2 subunits in mammalian cells assemble in high molecular weight complexes and associate with clathrin-coated vesicles (Phan et al., 1994; Stepp et al., 1995). In addition, disruption of several of these genes in combination with clathrin heavy chain (*CHC1*) mutations exacerbates some of the defects observed in *chc1* mutants. However, deletions of the genes encoding AP-1 and AP-2 homologs in a wild-type background result in no detectable defects in protein trafficking (Phan et al., 1994; Rad et al., 1995; Stepp et al., 1995).

Recently, a third AP complex (AP-3) was identified in mammalian cells that, like AP-1 and AP-2, is heterotetrameric, consisting of two large subunits (β3a and δ), a medium subunit (μ3a), and a small subunit (σ3) (Dell'Angelica et al., 1997; Simpson et al., 1997). However, unlike the previously characterized AP complexes, AP-3 does not associate with clathrin (Newman et al., 1995; Simpson et al., 1996). Furthermore, although yeast two-hybrid studies have shown that the μ3a subunit can interact with a cytoplasmic sorting signal (Dell'Angelica et al., 1997), a specific role for AP-3 in protein trafficking has not been defined.

In yeast, genetic screens have isolated >40 vacuolar protein-sorting (*vps*) mutants defective in localization of hydrolases from the Golgi to the vacuole (Bankaitis et al., 1986; Robinson et al., 1988; Rothman et al., 1989). Vacuolar delivery of most of the proteins that have been studied, including carboxypeptidase Y (CPY), proceeds via an endosomal intermediate (Vida et al., 1993). However, an alternative pathway from the Golgi has recently been found to transport alkaline phosphatase (ALP) to the vacuole in a manner that is independent of the *PEP12* (t-SNARE) and *VPS45* (Sec1p homolog) gene products required for vacuolar delivery of CPY (Cowles et al., 1997). In addition, vacuolar delivery of ALP is independent of several other *VPS* gene products, including Vps4p (endosomal AAA-ATPase) (Babst et al., 1997), the Vps15p protein kinase (Herman et al., 1991; Raymond et al., 1992), the Vps34p PtdIns 3-kinase (Stack et al., 1995), Vps8p (Horazdovsky et al., 1996), and Vac1p (Webb et al., 1997). Delivery of ALP to the vacuole via this alternative pathway is dependent upon a sorting signal contained within the cytoplasmic tail of ALP (Cowles et al., 1997), suggesting that a sorting mechanism regulates entry into the *PEP12/VPS45*-independent pathway.

We now describe the identification of the AP-3 complex in yeast that is required for cargo-selective transport of ALP to the vacuole/lysosome. Deletion of each subunit of the AP-3 complex results in mislocalization of ALP and the vacuolar t-SNARE, Vam3p, to a nonvacuolar compartment(s) but has no effect on the vacuolar transport of CPY or carboxypeptidase S (CPS). In addition, a green fluorescent protein (GFP)-ALP fusion protein, which is exclusively localized to the vacuolar membrane in wild-type cells, accumulates in numerous cytoplasmic vesicles and tubules in AP-3 deletion mutants. These studies, therefore, provide evidence that the AP-3 complex functions in transport to the vacuole/lysosome.

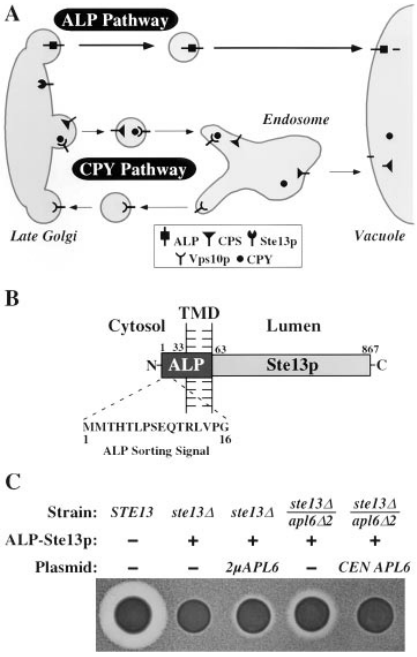

Figure 1. Genetic Screen for Transport Factors of the ALP Pathway Identifies Subunits of the Yeast AP-3 Adaptor Complex

(A) Schematic diagram of two distinct Golgi-to-vacuole transport pathways in yeast. The CPY pathway transports the soluble hydrolase CPY, bound to its receptor (Vps10p), and the integral membrane protein CPS from a late Golgi compartment to the vacuole via a prevacuolar endosome. An alternative route, the ALP pathway, is responsible for Golgi-to-vacuole delivery of the integral membrane protein ALP.

(B) The ALP-Ste13p fusion protein, consisting of the N-terminal cytoplasmic and transmembrane domains of ALP fused to the lumenal, enzymatically active C terminus of Ste13p.

(C) α factor halo assay. Cells of indicated genotypes were plated on a lawn of *MAT***a** *sst1* cells and scored for halo formation.

Results

Identification of Factors Specific for Transport to the Vacuole via the ALP Pathway

Two distinct pathways transport cargo proteins from the Golgi to the vacuole: the "CPY pathway" delivers CPY and CPS to the vacuole via a prevacuolar compartment and requires the *PEP12* and *VPS45* gene products, whereas the "ALP pathway" delivers ALP to the vacuole in a *PEP12/VPS45*-independent manner (Figure 1A). To identify components specific for ALP pathway delivery, a genetic screen was initiated that relies upon the ability of the ALP sorting determinant to localize Ste13p (dipeptidyl aminopeptidase A) to the vacuole. Ste13p is one of three resident late Golgi membrane proteins involved in the proteolytic maturation of the secreted mating pheromone α factor in *MAT*α cells (Julius et al., 1983; Fuller et al., 1988). Binding of secreted mature α factor to its receptor, Ste2p, on *MAT***a** cells causes a G_1 arrest of the cell cycle. Thus, secretion of mature α factor by wild-type (*STE13*) *MAT*α cells results in a zone of growth inhibition (halo) when these cells are plated on a *MAT***a** tester lawn (Sprague et al., 1981). Cells deleted for the *STE13* locus (*ste13*Δ), however, fail to secrete mature α factor and show no halo formation (Julius et al., 1983).

The cytoplasmic and transmembrane domains of ALP were fused to the proteolytically active lumenal domain of Ste13p (Figure 1B). The ALP-Ste13p fusion protein was incapable of restoring α factor halo formation to *ste13*Δ cells (Figure 1C), consistent with localization of this chimera to the vacuole. We reasoned that overexpression of factors critical for transport of ALP to the vacuole might cause a dominant negative phenotype resulting in mislocalization of ALP-Ste13p to the Golgi, thereby increasing α factor maturation and enhancing halo formation. *ste13*Δ cells containing a plasmid encoding ALP-Ste13p were transformed with a high copy (2μ) genomic library and screened for enlarged α factor halos. As expected, two of the eight library plasmids isolated within the first 15,000 colonies screened contained 2μ *MF*α (α factor) or *STE13* (data not shown). However, a subtle halo enhancement was observed in cells harboring 2μ plasmids containing either *APL6/YKS5* (Figure 1C) or *APL5/YKS4* (data not shown). Deletion of *APL6* in *ste13*Δ cells resulted in a more pronounced halo enhancement that could be complemented by introduction of *APL6* on a single-copy (*CEN*) plasmid (Figure 1C). These results suggest that overproduction of either *APL6* or *APL5* interferes with the delivery of ALP from the Golgi to the vacuole.

An examination of the Saccharomyces Genome Database revealed that *APL6* (ORF YGR261C) and *APL5* (ORF YPL195W) are predicted to encode proteins homologous to AP subunits identified in both yeast and mammalian cells. The phylogenetic relationships between yeast and mammalian APs were investigated by comparison of the primary structures of these proteins. A progressive alignment of the amino acid sequences of the large, medium, and small APs yielded similarity scores and pairwise distances that were converted into dendrograms by BLOSUM matrix analysis (Feng and Doolittle, 1996). As shown in Figure 2A, the *APL6* gene product (Apl6p) displays highest homology with β3a adaptin, and the *APL5* gene product (Apl5p) is most closely related to δ adaptin. Both β3a and δ have recently been identified as the large subunits of a novel, ubiquitously expressed AP-3 complex in mammalian cells (Simpson et al., 1997), suggesting that Apl6p and Apl5p are the large subunits of a homologous complex in yeast. Alignment also showed that Apl4p is homologous to AP-1 γ and Apl3p is homologous to AP-2 α. Due to the high degree of identity (84%) between β1 and β2, however, Apl1p and Apl2p could not be paired with their respective mammalian homologs.

The identification of Apl6p and Apl5p as homologs of β3a and δ suggested that yeast APs homologous to μ3a and σ3 would correspond to the medium and small subunits, respectively, of an AP-3 complex in yeast. Progressive alignment identified Apm3p as the homolog of μ3a, as well as Apm1p and Apm4p as homologs of μ1 and μ2, respectively (Figure 2A). Interestingly, a fourth medium AP subunit in yeast, Apm2p, diverged much earlier and does not yet appear to have a corresponding mammalian homolog in the database. Alignment of the small APs identified Aps3p as the homolog of σ3, whereas Aps1p and Aps2p are homologs of σ1 and σ2, respectively (Figure 2A). These phylogenetic analyses,

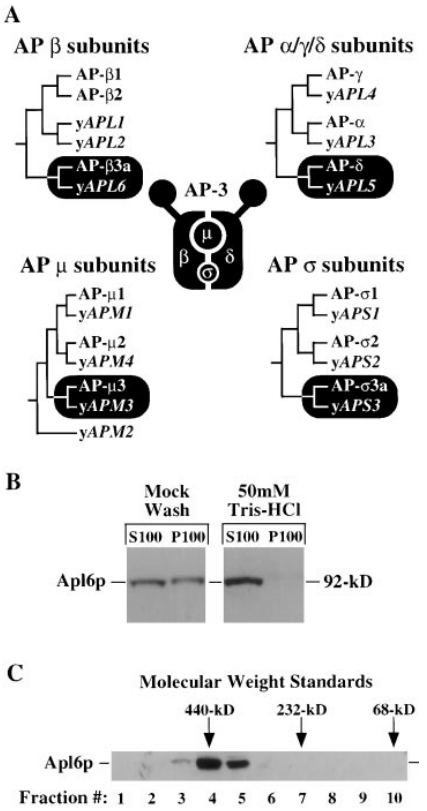

Figure 2. Apl6p Is a Peripheral Membrane-Associated Component and Part of a High Molecular Weight Complex

(A) Phylogenetic analysis of yeast and mammalian AP complex subunits. The mammalian AP-3 subunits and their yeast homologs are highlighted in black.

(B) Wild-type spheroplasts were lysed and treated with either a mock wash or a 50 mM Tris-HCl (pH 7.5) wash then centrifuged at 100,000 × g to produce pellet (P100) and supernatant (S100) fractions. Samples were resolved by SDS-PAGE, and Apl6p was visualized by immunoblotting and ECL.

(C) The elution profile of Apl6p in wild-type S100 fractions loaded over a Sephacryl S-300 column was visualized by SDS-PAGE and immunoblotting. Elutions of the molecular weight standards ferritin (440 kDa), ADH (232 kDa), and BSA (68 kDa) are indicated.

therefore, identify AP complexes in yeast that are homologous to the AP-1, AP-2, and AP-3 complexes in mammalian cells with the yeast AP-3 complex comprised of Apl6p, Apl5p, Apm3p, and Aps3p.

Components of the AP-1 and AP-2 complexes are found in both soluble cytosolic and membrane-associated pools (Robinson, 1994), indicative of a functional cycle of membrane binding and dissociation during vesicular budding. Antiserum was raised against Apl6p, and spheroplasts from wild-type cells were lysed then subjected to differential centrifugation to generate membrane-enriched P13 (13,000 × g) and P100 (100,000 × g) fractions and a soluble cytosolic S100 fraction. The P13 fraction contains vacuole, ER, and plasma membranes (Marcusson et al., 1994), whereas the P100 fraction is enriched for membranes of the Golgi apparatus, endosome, and transport vesicles (Vida et al., 1993; Marcusson et al., 1994). Immunoblotting showed that Apl6p is equally distributed between the cytosolic fraction and the high speed (P100) membrane pellet (Figure 2B). In addition, treatment of cell lysates with 50 mM Tris-HCl (pH 7.5) resulted in the displacement of membrane-associated Apl6p to the cytosolic fraction (Figure 2B), consistent with the recent characterization of σ3, which revealed that its membrane association could be disrupted by Tris-HCl (Dell'Angelica et al., 1997). Thus, Apl6p exists in both a soluble cytosolic pool and a peripherally associated membrane-bound pool. Furthermore, in S100 fractions eluted from a sizing column (Figure 2C), Apl6p coeluted with the 440 kDa molecular weight marker ferritin (fraction 4), whereas no monomeric Apl6p could be detected (fractions 9 and 10), consistent with Apl6p assembling as a component of a high molecular weight complex.

Deletions of AP-3 Subunits Result in Specific Defects in the ALP Pathway

The role of the predicted AP-3 complex in the vacuolar transport of ALP was directly addressed by deletion of either *APL6*, *APL5*, *APM3*, or *APS3* followed by pulse-chase metabolic labeling and immunoprecipitation. ALP is transported through the secretory pathway as a 74 kDa precursor (proALP) that, upon delivery to the vacuole, is activated by proteolytic cleavage near its C terminus to yield the mature 72 kDa form (mALP). In wild-type cells, newly synthesized ALP was rapidly delivered to the vacuole, as complete maturation occurred within 30 min (Figure 3A). Strikingly, deletion of any of the four predicted AP-3 subunits strongly impaired ALP maturation (Figure 3A). In addition, proALP migrated with a slightly slower electrophoretic mobility in each of the four AP-3 deletion mutants (Figure 3A) due to increased elongation of N-linked oligosaccharides on the lumenal domain of the protein (data not shown). Interestingly, a more extensively processed form of ALP (denoted by an asterisk in Figure 3C) that is found in low amounts in wild-type cells after an extended chase time of 60 min is more abundant in *apl5Δ1* cells (Figure 3C). Processing of ALP in AP-3 mutant cells was *PEP12*-dependent and *SEC1*-independent (data not shown), suggesting that some ALP transits the CPY pathway in the absence of AP-3 function.

Vacuolar delivery of ALP does not require AP-1 or AP-2, as ALP was found to be matured with wild-type kinetics in cells deleted for both *APL1* and *APL2* (Figure 3A) as well as both *APS1* and *APS2* (data not shown). To address whether the AP-3 complex is required for transport along the CPY pathway, the vacuolar delivery of CPS was examined. Like ALP, CPS is a type II membrane protein transported through the secretory pathway as an inactive precursor (proCPS). Once localized to the vacuole, CPS is cleaved at a site just lumenal to the transmembrane domain to yield a soluble active form of the enzyme (mCPS) (Spormann et al., 1992). In contrast to ALP, however, CPS is delivered from the Golgi to the vacuole via the CPY pathway (Cowles et al., 1997). As shown in Figure 3A, maturation of newly synthesized CPS was nearly complete within 30 min in wild-type cells and proceeded with wild-type kinetics in cells in which any of the four AP-3 subunits had been deleted (Figure 3A). Neither AP-1 nor AP-2 was required

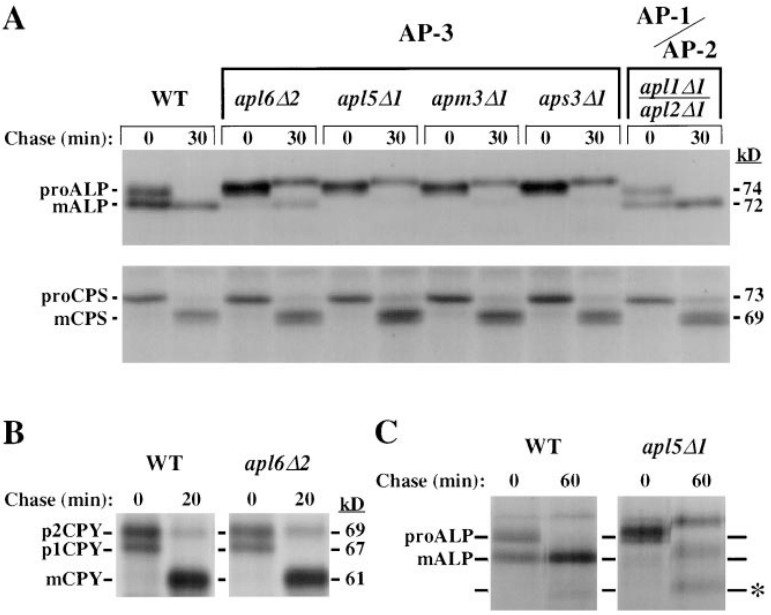

Figure 3. Deletions of AP-3 Subunits Result in Specific Defects in Vacuolar Delivery of ALP

Cells were labeled for 10 min then chased for 0 or 30 min and lysed. (A) ALP, CPS, and (B) CPY were isolated by immunoprecipitation and resolved by SDS-PAGE. (C) Wild-type (WT) and *apl5Δ1* cells were labeled and chased for 0 and 60 min, then ALP was immunoprecipitated. An additional processed form of ALP is indicated by an asterisk.

for transport of CPS to the vacuole, although processing of CPS was slightly delayed in cells deleted for both *APL1* and *APL2* (Figure 3A) or for other AP-1 and AP-2 subunits (data not shown). In addition, vacuolar delivery of CPY was found to be normal in the absence of AP-3 function (Figure 3B). Thus, AP-3 is specifically required for transport via the ALP pathway.

ALP and the Vacuolar t-SNARE, Vam3p, Are Mislocalized to a Nonvacuolar Compartment in AP-3 Mutant Cells

The fate of newly synthesized ALP in AP-3 deletion mutants was investigated further in spheroplasts of wild-type and *apl6Δ2* cells that were pulse labeled and chased for 30 min then lysed and subjected to subcellular fractionation and immunoprecipitation. As shown in Figure 4A, in wild-type cells, newly synthesized ALP was found almost exclusively in its mature form in the P13 fraction containing vacuolar membranes. In contrast, >60% of proALP was found in the P100 membrane pellet in *apl6Δ2* cells. Approximately 30% of ALP could be detected in the P13 pellet, suggesting that a fraction of newly synthesized ALP had been delivered to the vacuole in AP-3 deletion mutants (Figure 4A).

The compartmental localization of newly synthesized ALP was examined further by equilibrium density gradient analysis. Labeled spheroplasts from wild-type and *apl6Δ2* cells were lysed and cleared of unbroken cells then loaded at the top of Accudenz density gradients and centrifuged to equilibrium. Fractions were collected from the top of each gradient and analyzed by immunoprecipitation. In wild-type cells, newly synthesized ALP was found exclusively in its mature form in the top fractions of the gradient (Figure 4B). In *apl6Δ2* cells, however, ALP was predominantly found in precursor form and sedimented in much denser fractions within the gradient (Figure 4B). This distribution of proALP in *apl6Δ2* cells was similar to the distribution in both wild-type and *apl6Δ2* cells of Kex2p and Vps10p (the sorting receptor for CPY), which cycle between the Golgi apparatus and the endosome (Figure 4C) (Marcusson et al., 1994). A fraction of newly synthesized ALP in *apl6Δ2* cells was found in its mature form at the top of the gradient (Figure 4B), consistent with a portion of ALP being delivered to the vacuole (Figure 4A). Thus, in the absence of AP-3 function, newly synthesized ALP accumulates in its precursor form within a dense nonvacuolar membrane-bound compartment.

The specific defects observed in the vacuolar transport of newly synthesized ALP suggest that the vacuolar delivery of other proteins via the ALP pathway might be impaired in AP-3 deletion mutants. One candidate cargo protein for the ALP pathway is Vam3p, a t-SNARE that functions at a late stage in vacuolar transport (Darsow et al., 1997; Wada et al., 1997), since the vacuolar localization of Vam3p is unchanged in *pep12* mutant cells (data not shown). The distribution of Vam3p was examined by gradient fractionation of wild-type and *apm3Δ1* cells followed by immunoblotting. As expected, the vast majority of Vam3p in wild-type cells colocalizes with mALP (Figure 5) and the 100 kDa subunit of the vacuolar ATPase (data not shown) in the top fractions of the gradient. In *apm3Δ1* cells, however, the distribution of Vam3p is dramatically altered, with equal amounts observed in the light vacuolar membrane fraction as well as a dense membrane fraction (Figure 5A) that also contains proALP (Figure 5B). A similar distribution of Vam3p and ALP was also seen in gradient fractions of *apl6Δ2* cells (data not shown). Thus, the normal vacuolar localization of Vam3p requires AP-3 function, suggesting that Vam3p is an ALP pathway cargo protein.

A GFP-ALP Fusion Protein Accumulates in Cytoplasmic Vesicles and Tubules in AP-3 Mutant Cells

The biochemical fractionation studies described above indicate that ALP and Vam3p are mislocalized to a nonvacuolar compartment upon deletion of either *APL6* or

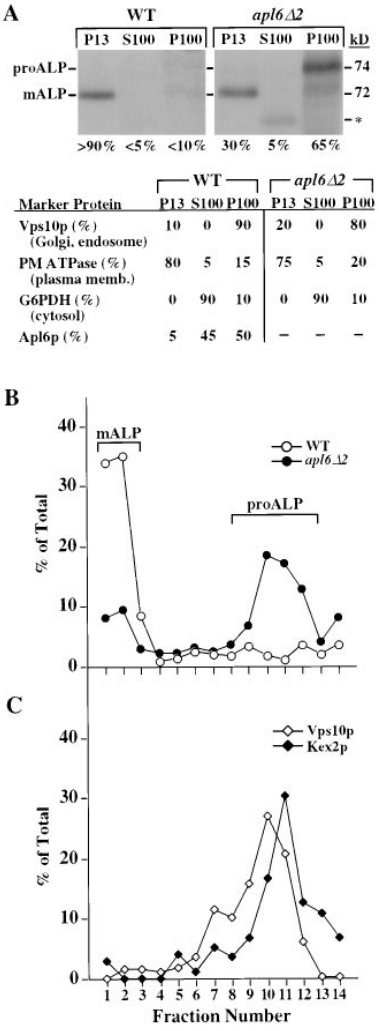

Marker Protein	WT P13	WT S100	WT P100	apl6Δ2 P13	apl6Δ2 S100	apl6Δ2 P100
Vps10p (%) (Golgi, endosome)	10	0	90	20	0	80
PM ATPase (%) (plasma memb.)	80	5	15	75	5	20
G6PDH (%) (cytosol)	0	90	10	0	90	10
Apl6p (%)	5	45	50	–	–	–

Figure 4. ALP Is Mislocalized in *apl6Δ2* Cells

(A) Wild-type (WT) and *apl6Δ2* spheroplasts were labeled for 30 min and chased for 30 min at 30°C then lysed and sequentially centrifuged to generate P13 (13,000 × g pellet), P100 (100,000 × g pellet), and S100 (100,000 × g supernatant) fractions. Proteins were immunoprecipitated, analyzed by SDS-PAGE, and quantitated by phosphorimage analysis.

(B and C) Wild-type and *apl6Δ2* spheroplasts were labeled for 15 min and chased for 30 min at 30°C. Cleared lysates were then loaded at the top of identical Accudenz gradients and centrifuged to equilibrium. Fourteen fractions were collected from the top, and proteins were immunoprecipitated, analyzed by SDS-PAGE, and quantitated by phosphorimage analysis. The distributions of Kex2p and Vps10p shown in (C) are the average of the distributions seen in wild-type and *apl6Δ2* cells, which did not differ significantly.

APM3. To investigate the nature of the compartment(s) in which cargo proteins of the ALP pathway accumulate in AP-3 mutant cells, GFP was fused to the cytoplasmic domain of ALP (Figure 6A). Like native ALP, maturation of newly synthesized GFP-ALP occurred rapidly in wild-type cells but was blocked in *apm3Δ1* cells (Figure 6A). In addition, GFP-ALP migrated with a slightly slower electrophoretic mobility after a 30 min chase in *apm3Δ1* cells. Thus, the trafficking of the GFP-ALP fusion protein accurately represents native ALP. In wild-type cells, fluorescence microscopy showed that GFP-ALP is exclusively located on the vacuolar membrane (Figure 6B).

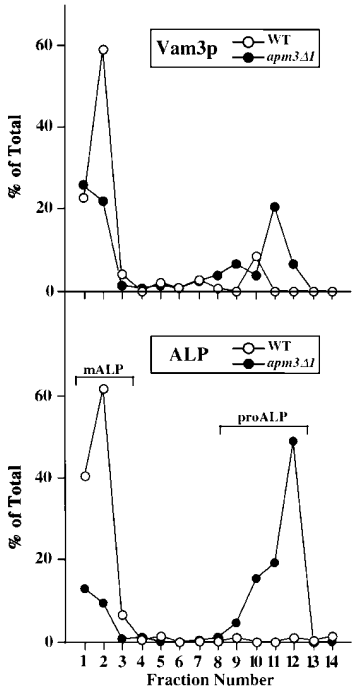

Figure 5. The Vacuolar t-SNARE Vam3p Is Mislocalized in *apm3Δ1* Cells

Spheroplasts from wild-type (WT) and *apm3Δ1* cells were lysed and fractionated on Accudenz gradients as described in the legend to Figure 4. The distributions of Vam3p and ALP, analyzed by SDS-PAGE and immunoblotting, were quantitated using NIH Image 1.59. The vacuolar membrane distribution of the 100 kDa subunit of the vacuolar ATPase was unaffected in *apm3Δ1* cells (data not shown).

In contrast, deletion of *APM3* resulted in a pronounced accumulation of GFP-ALP in cytoplasmic vesicles (Figure 6B) as well as a population of tubules that were often up to 1 μm in length (Figure 6B, arrow). In addition, GFP-ALP was found on the vacuolar membrane in *apm3Δ1* cells (Figure 6B), which was dependent upon a functional CPY pathway, as no fluorescence on the vacuole was detected upon simultaneous deletion of *VPS4* in *apm3Δ1* cells (data not shown).

To determine whether the AP-3 complex is required for normal vacuolar assembly, uptake of the vital fluorescent lipophilic styryl dye FM 4-64 was examined. FM 4-64 is endocytosed from the plasma membrane to the vacuole in a time-, temperature-, and energy-dependent manner (Vida and Emr, 1995). Wild-type and *apl6Δ2* cells were incubated with FM 4-64 for 15 min at 30°C to allow incorporation of the dye into the plasma membrane then washed to remove unbound dye and chased for 45 min at 30°C. In both wild-type and *apl6Δ2* cells, FM 4-64 exclusively labeled the vacuolar membrane after a 45 min chase (Figure 6C). Vacuolar staining was evident within 15 min of chase in both wild-type and *apl6Δ2* cells (data not shown). Therefore, the AP-3 complex is not required for vacuolar assembly despite its role in cargo-selective Golgi-to-vacuole transport. In addition, the normal uptake of FM 4-64 in *apl6Δ2* cells indicates that the AP-3 complex is not essential for endocytic membrane transport to the vacuole.

The accumulation of GFP-ALP within cytoplasmic

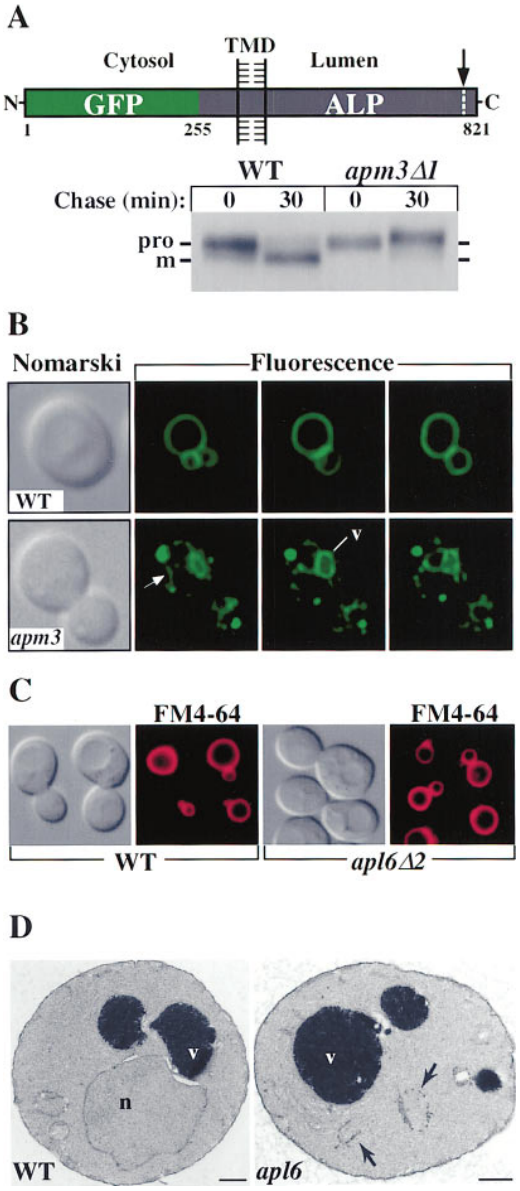

Figure 6. A GFP-ALP Fusion Protein Is Mislocalized in AP-3 Mutants

(A) Schematic diagram and processing of the GFP-ALP chimera. Wild-type and *apm3Δ1* cells were labeled for 10 min, chased for 0 or 30 min, and GFP-ALP was immunoprecipitated from lysates with anti-ALP antiserum.

(B) Nomarski optics and fluorescence localization of GFP-ALP in wild-type and *apm3Δ1* cells shown in serial 200 nm sections. A similar distribution of GFP-ALP was also seen in *apl6Δ2* cells (data not shown).

(C) FM 4-64 localization in wild-type and *apl6Δ2* cells incubated for 15 min with FM 4-64 then chased for 45 min and viewed with Nomarski optics and fluorescence.

(D) Sections of wild-type and *apl6Δ2* cells viewed by electron microscopy. Wild-type and *apl6Δ2* cells were grown at 30°C and fixed with glutaraldehyde. Arrows, accumulated membrane structures; n, nucleus; v, vacuole; bars, 0.5 μm.

vesicles and tubules of AP-3 mutant cells suggests that in the absence of AP-3 function, aberrant structures could form, within which ALP accumulates. Alternatively, the cargo-selective block in Golgi-to-vacuole delivery via the ALP pathway might prolong the residence of ALP in the Golgi and/or transport intermediates and result in subsequent transport via the CPY pathway. Wild-type and *apl6Δ2* cells were examined by electron microscopy to determine whether AP-3 mutant cells exhibit an abnormal cellular morphology. In wild-type cells, nuclei and vacuoles are surrounded by cytoplasm that is relatively clear of other membrane structures (Figure 6D). In *apl6Δ2* cells, however, an accumulation of vesicles and tubules was observed, although no disparity of vacuolar structure was detected (Figure 6C). A similar increase in cytoplasmic membrane structures was also observed in *apm3Δ1* cells (data not shown).

Discussion

A gene dosage-dependent screen designed to detect missorting of an ALP-Ste13p fusion protein has revealed a role for the AP-3 adaptor complex in cargo-selective protein transport from the Golgi to the vacuole in yeast. Two gene products identified using this genetic screen, Apl6p and Apl5p, are homologs of β3a adaptin and δ adaptin of the heterotetrameric AP-3 complex recently identified in mammalian cells (Dell'Angelica et al., 1997; Simpson et al., 1997). Deletion of *APL6*, *APL5*, or the medium (μ3a) or small (σ3) AP-3 subunit homologs (*APM3* and *APS3*, respectively) results in a specific defect in vacuolar delivery of newly synthesized ALP and in a dramatic mislocalization of both ALP and the vacuolar t-SNARE Vam3p, while transport of other vacuolar cargo proteins, including CPS and CPY, is unaffected. Furthermore, a GFP-ALP fusion protein, which localizes to the vacuolar membrane in wild-type cells, accumulates in vesicles and tubules in AP-3 deletion mutants. These results implicate the AP-3 complex as a critical component of the alternative Golgi-to-vacuole transport pathway (the ALP pathway) recently identified in S. cerevisiae (Cowles et al., 1997).

The observation that *APL6* and *APL5* encode homologs of the β3a and δ adaptins of the mammalian AP-3 complex strongly suggests the existence of a homologous AP-3 complex in yeast. Accordingly, Apl6p and Apl5p are anticipated to associate in a heterotetramer with a medium and small AP subunit, predicted by phylogenetic analysis to be Apm3p and Aps3p, respectively. Indeed, deletion of either *APL6*, *APL5*, *APM3*, or *APS3* specifically impaired vacuolar delivery of ALP but not of CPS and CPY. The Apl6 protein is distributed equally between membrane-associated and soluble pools and is detected in a high molecular weight complex. The simplest interpretation of these results is that AP-3 is a peripherally associated coat complex involved in vesicle budding and packaging of specific cargo proteins. Furthermore, neither the CPY pathway nor the ALP pathway requires AP-1 or AP-2 subunits. Thus, the AP-3 adaptor complex in yeast fulfills an important role in cargo-selective transport from the Golgi to the vacuole.

Unlike the AP-1 and AP-2 complexes, which function in protein sorting at the TGN and plasma membrane, respectively, a role for AP-3 in protein trafficking in mammalian cells has yet to be established. Recent studies have localized the mammalian AP-3 complex to both late Golgi and endosomal membranes (Dell'Angelica et

al., 1997; Simpson et al., 1997). Additionally, the observation that the δ AP-3 subunit is the mammalian homolog of the *garnet* gene of Drosophila melanogaster has been invoked to argue in favor of a role for AP-3 in transport to the lysosome (Simpson et al., 1997). *garnet* mutant flies exhibit defects in pigment granule biogenesis, a process thought to be analogous to lysosomal biogenesis (Burkhardt et al., 1993; Simpson et al., 1997). A correlation between Drosophila eye color phenotype and lysosomal transport is further substantiated by the observation that the *VPS18* gene, which is required for protein transport to the vacuole (Robinson et al., 1991), is the yeast homolog of *deep orange*, another Drosophila eye color gene (Reider and Emr, submitted). In mammalian cells, pigment granules also appear to be related to lysosomes, as patients with Chediak-Higashi syndrome (related to the *beige* mutant in mice) exhibit enlarged lysosomes and melanosomes (Burkhardt et al., 1993). A specific functional role for AP-3 in protein sorting to the vacuole/lysosome is now provided by the observation that AP-3 is required for cargo-selective Golgi-to-vacuole transport. The finding that AP-3 is specifically required for vacuolar delivery via the ALP pathway suggests that this alternative Golgi-to-vacuole route (Cowles et al., 1997) is homologous to the pathway followed by proteins (e.g., pigment transporters) required for pigment granule formation in Drosophila.

This discovery provides significant insight into the mechanisms regulating Golgi-to-vacuole/lysosome transport. In mammalian cells, AP-1 and AP-2 adaptor complexes associate at the cytoplasmic face of the TGN and plasma membrane, respectively, where they selectively concentrate signal-bearing membrane proteins into clathrin-coated pits (Marks et al., 1997; Robinson, 1997). Unlike AP-1 and AP-2, however, studies have clearly shown that AP-3 in mammalian cells does not copurify with clathrin-coated vesicles (Simpson et al., 1996). Similarly, vacuolar delivery of ALP is not affected by deletion of the clathrin heavy chain gene (*CHC1*) in yeast (Seeger and Payne, 1992). A model of AP-3 function, therefore, involves direct participation in cargo-selective packaging of ALP and Vam3p into transport vesicle intermediates surrounded by a nonclathrin coat. By analogy with AP-1 and AP-2, the yeast AP-3 complex is predicted to recognize a sorting determinant contained within the cytoplasmic domains of transmembrane cargo proteins. A region of the cytoplasmic tail of ALP that contains a di-leucine-type motif has been identified by deletion analysis to be essential for vacuolar delivery (Cowles et al., 1997). In mammalian cells, di-leucine-based signals target membrane proteins from the TGN and the plasma membrane to the lysosome (Letourneur and Klausner, 1992) and interact with both AP-1 and AP-2 complexes in vitro (Heilker et al., 1996). Potential di-leucine-based signals can also be found in the cytoplasmic domain of Vam3p. Thus, the AP-3 complex may also interact with a subset of di-leucine-based signals to mediate entry of cargo proteins into the ALP pathway.

Presently, our data suggest that AP-3 functions at a late Golgi compartment, since a deletion of any of the four predicted AP-3 subunits results not only in a selective block in vacuolar delivery of newly synthesized ALP but also in hyperglycosylation, indicative of a prolonged exposure of ALP to oligosaccharide modifying enzymes present in the Golgi complex. Furthermore, gradient fractionation studies indicate that in AP-3 mutant cells, proALP and Vam3p accumulate in a dense membrane fraction coincident with the normal distribution of the late Golgi proteins Kex2p and Vps10p (the CPY sorting receptor), which cycle between the endosome and Golgi (Wilcox et al., 1992; Nothwehr et al., 1993; Marcusson et al., 1994). The numerous vesicles and tubules that accumulate GFP-ALP in AP-3 mutant cells are likely to correspond to compartments of the Golgi and transport intermediates. In addition, the subtle increase in membrane structures in the cytoplasm of AP-3 mutants seen by electron microscopy suggests that GFP-ALP may also accumulate in aberrant structures in the absence of AP-3 function.

The subunits of the yeast AP-3 complex were recently isolated as suppressors of temperature-sensitive yeast casein kinase (*yck*) mutations; however, the mechanism of suppression or role in casein kinase signaling of AP-3 is unclear (Panek et al., 1997). A role for AP-3 in endocytosis is unlikely, as endocytic transport of both the yeast pheromone receptor Ste3p (Panek et al., 1997) and FM 4-64 is unaffected by deletion of AP-3 subunits. We have identified the Apl6 and Apl5 proteins exclusively on the basis of their involvement in the ALP pathway. Previously, only Vps41p had been shown to function preferentially in ALP vacuolar transport (Cowles et al., 1997). However, *vps41*Δ mutants exhibit more severe defects, including fragmented vacuoles and endosomes and secretion of CPY (Radisky et al., 1997), suggesting that Vps41p functions at a later step in the ALP pathway than does the AP-3 complex. Given the established role of Vam3p in the vacuolar delivery of both ALP pathway and CPY pathway cargo proteins (Darsow et al., 1997; Wada et al., 1997), it is surprising that mislocalization of Vam3p in AP-3 mutant cells does not result in a CPY pathway block and/or gross morphological defects. Recent studies, however, suggest that Vam3p can be mislocalized to the CPY pathway when overexpressed (Darsow et al., 1997). Thus, it is likely that a sufficient amount of Vam3p enters the CPY pathway in AP-3 mutants to maintain a functional pool of Vam3p at the vacuole. Our results, therefore, suggest that distinct sorting pathways from the late Golgi are responsible for the segregation of the vacuolar t-SNARE Vam3p and the endosomal t-SNARE Pep12p. It is also likely that some ALP enters the CPY pathway in the absence of AP-3 function, as a fraction of ALP is localized to the vacuole in AP-3 mutant cells in a manner that is dependent upon the *PEP12* and *VPS4* gene products.

The identification of a requirement for yeast AP-3 function in the ALP pathway to the vacuole underscores the power of yeast as a model system for the study of AP complex function. Considering the homology that exists between mammalian and yeast AP-3 complexes and the similar properties of yeast and mammalian transport systems, a Golgi-to-lysosome pathway comparable to the ALP pathway is likely to exist as the site of function for mammalian AP-3. Furthermore, an overtly detectable phenotype associated with disruption of the AP-3 complex in yeast now exists, and expansion of the screen for ALP pathway-specific factors should continue to identify other proteins involved in this alternative Golgi-to-vacuole pathway. Continued characterization

of AP-3 and other ALP pathway components is anticipated to provide additional insights into the reasons for this alternative vacuolar delivery pathway as well as the molecular mechanisms that underlie the packaging, docking, and fusion of transport vesicles.

Experimental Procedures

Materials and Plasmid Constructions

Media and reagents are identical to those described previously (Cowles et al., 1997). A bacterially expressed GST fusion protein containing 159 amino acids of Apl6p encoded by a BglII-BglII DNA fragment was purified and used to immunize New Zealand white rabbits as previously described (Horazdovsky and Emr, 1993). Purified GST-Apl6p coupled to CNBr-activated Sepharose (Pharmacia) was used to affinity purify anti-Apl6p antiserum.

The ALP-Ste13p fusion protein was constructed by PCR using gene Splicing by Overlap Extension (gene SOE) (Yon and Fried, 1989) using templates pALP1 (Cowles et al., 1997) and pDA6300 (*STE13*; D. Barnes) with oligonucleotides ALP5′ (Cowles et al., 1997), AS3′ (5′-GGTAGGTAGAAGTTTTGATGCAGAACGTAATGC-3′), AS5′ (5′-TTACGTTCTGCATCAAAACTTCTACCTACCAAAATC-3′), and SPRUNG (5′-GATGGGTATCATCACCGCCC-3′). The resulting 3 kb gene fusion was ligated with pCRII (Invitrogen) then excised via EcoRI digestion and ligated with pRS414 (Sikorski and Hieter, 1989), resulting in pAS13.

Isolated library plasmid pCC300 was cleaved with SacI and NarI to release a 3.8 kb fragment containing *APL6*. This fragment was ligated with pRS416, pRS426 (Sikorski and Hieter, 1989), and pBluescriptSK$^+$ (Stratagene) to yield pCC301, pCC302, and pCC303, respectively. pCC303 was digested with NheI, filled with Klenow DNA polymerase, cleaved with NsiI to remove a 5′ portion of *APL6* coding sequence, and ligated with an EcoRI (fill)-PstI-digested fragment containing the *HIS3* gene, creating the *APL6* disruption plasmid pCC304.

For construction of the GFP-ALP fusion protein, plasmid pS65T (Clontech) was used with primers GO21p and GO22p as a template for PCR to generate an 814 bp fragment that includes the start codon of GFP and the 3′ polylinker of pS65T. A 495 bp fragment consisting of the CPY 5′UTR was generated by PCR using the plasmid pCYI50 as a template with primers GO19p and GO20p. Gene SOE was used to fuse the CPY 5′UTR upstream of GFP (S65T) to generate the N-terminal GFP fusion construct pGOGFP. pGOGFP was subcloned into pRS426 and digested with KpnI. The plasmid pALP1 was used as a template with primers GO25p and GO26p to generate a 1.9 kb fragment that placed a KpnI site at the start of the ALP coding region. This fragment was subcloned into pCRII (Invitrogen) then excised as a KpnI fragment and ligated with pGOGFP in pRS426.

Phylogenetic Analysis of APs

The Saccharomyces Genome Database was searched for proteins with homology to Apl6p and Apl5p, which identified the set of yeast and mammalian APs shown in Figure 2A. For phylogenetic analysis, the protein sequences of the yeast and mammalian APs were first cropped to standardize their lengths then compared by progressive alignment (Feng and Doolittle, 1996). The resulting pairwise distributions and similarities were scored with a BLOSUM matrix and converted to dendrograms using a Tree Draw program.

Genetic Manipulations

Standard yeast genetic procedures were used (Sherman et al., 1979). CCY250 (*ste13*Δ) cells were generated via transformation of SEY6210 cells (*MAT*α *leu2-3,112 ura3-52 his3-*Δ*200 trp1-*Δ*901 lys2-801 suc2-*Δ*9*) (Robinson et al., 1988) with a *ste13*Δ*::LEU2*-containing fragment of pSL349 (Nothwehr et al., 1993). Leu$^+$ colonies were selected and confirmed to be deficient for halo formation when tested for α factor production. CCY255 (*apl6*Δ*2*) cells were created via transformation of SEY6210 cells with SphI-SacI-digested pCC304. His$^+$ colonies were selected and confirmed to contain a genomic disruption of *APL6* by PCR. Genomic deletion of the remaining AP-3 subunits was achieved by construction of *HIS3* PCR fragments (Baudin et al., 1993) using primers containing a 5′ overhang identical to the first 50 bases of the N-terminal coding regions and a 3′ overhang complementary to the last 50 bases of the C-terminal coding regions, respectively, of either *APL5*, *APM3*, or *APS3*. His$^+$ colonies of SEY6210 cells transformed with the resulting deletion constructs were confirmed to contain a genomic deletion by PCR of isolated genomic DNA. Disruptions of *APL1*, *APL2*, *APS1*, and *APS2* have been described (Phan et al., 1994; Rad et al., 1995).

α Factor Halo Assay Screen

CCY250 (*ste13*Δ) cells harboring pAS13 (ALP-Ste13p) were transformed with a high copy genomic library (2μ, *URA3*; M. Rose) and plated to Ura-selective SD plates at a transformant density of approximately 200 colonies/plate. Ura$^+$ transformants were replica plated to halo test plates generated by overlay of Ura-selective SD plates containing casamino acids with an 8 ml agar suspension of 0.6 A_{600} units of RC634 cells (*MAT***a** *sst1-3 ase2 his6 met1 ura1 rme1*) (Chan and Otte, 1982) harboring pRS426. Colonies showing enhanced α factor halo production were selected, and library plasmids were isolated and sequenced (Sanger et al., 1977).

Immunoprecipitation and Subcellular Fractionation

Cell labeling and immunoprecipitations were performed as previously described (Cowles et al., 1997), with EXPRE^{35}S^{35}S label (NEN/DuPont) incubations proceeding for 10 min prior to addition of methionine, cysteine, and yeast extract to final concentrations of 5 mM, 1 mM, and 0.2%, respectively, for indicated chase durations. ALP, CPS, and CPY in each lysate were immunoprecipitated. Endoglycosidase H treatment was performed on all CPS samples as previously described (Cowles et al., 1997).

Subcellular fractionations were performed as previously described (Cowles et al., 1997), with labeling proceeding for 30 min at 30°C prior to a 30 min chase at 30°C. Protein amounts in each fraction were determined by immunoprecipitation. Washes of S13 fractions with 50 mM Tris-HCl were for 30 min on ice. An equal volume of mock wash buffer (0.2 M sorbitol, 2 mM EDTA, 20 μg/ml PMSF, 5 μg/ml antipain, 1 μg/ml aprotinin, 0.5 μg/ml leupeptin, 0.7 μg/ml pepstatin, 10 μg/ml α_2-macroglobulin) or 2× Tris-HCl wash buffer (100 mM Tris-HCl [pH 7.5] in mock wash buffer) was added to each S13 fraction. Treated fractions were then centrifuged at 100,000 × g for 1 hr, S100 and P100 fractions were generated, and immunoblotting with anti-Apl6p antiserum was performed at a 1:1250 dilution and visualized by ECL (Amersham).

For gradient fractionation, 25 A_{600} units of SEY6210 or CCY255 cells were pulse labeled for 15 min and chased for 30 min at 30°C then spheroplasted and lysed as described previously (Cowles et al., 1997). The lysates were cleared of unbroken cells at 500 × g then loaded at the top of identical gradients and centrifuged to equilibrium in a Beckman SW41 rotor for 18 hr at 170,000 × g at 4°C. Gradient solutions were prepared in lysis buffer (0.2 M sorbitol, 50 mM KOAc, 20 mM HEPES [pH 6.8], 2 mM EDTA, 20 μg/ml PMSF, 5 μg/ml antipain, 1 μg/ml aprotinin, 0.5 μg/ml leupeptin, 0.7 μg/ml pepstatin, 10 μg/ml α_2-macroglobulin) and generated with the following weight/volume amounts of Accudenz (Accurate Chemical and Scientific Corp.): 1 ml 43%, 1 ml 37%, 1 ml 31%, 1.5 ml 27%, 1.5 ml 23%, 1.5 ml 20%, 1 ml 17%, 1 ml 13%, and 1 ml 8%. Following centrifugation, fourteen fractions were collected from the top, and the Accudenz concentration was determined by measuring the refractive index. Total protein from each fraction was precipitated in 10% TCA. Immunoprecipitations were quantitated by phosphorimage analysis (Molecular Dynamics). Immunoblotting was quantitated using NIH Image 1.59.

S100 Sizing Column Analysis

One thousand A_{600} units of TVY614 cells were spheroplasted, dounce homogenized, and pelleted at 100,000 × g. Resulting supernatant protein (11 mg) was loaded over a Sephacryl S-300 column (Pharmacia) in a running buffer consisting of 0.1 M potassium acetate, 20 mM HEPES (pH 7.2), 0.5 mM DTT, 2 mM magnesium acetate. Eluted fractions were immunoblotted with anti-Apl6p antiserum at 1:5000 dilution and visualized by ECL. The sizing column was standardized with blue dextran, ferritin, ADH, and BSA.

Microscopy

For GFP-ALP fluorescence analysis, 4 A_{600} units of exponentially growing cells were centrifuged at 500 × g and resuspended in 100 μl of YPD. Images of serial 200 nm sections were collected on a fluorescence microscope equipped with a FITC filter and deconvolved using Delta Vision software on a Silicon Graphics workstation.

For FM 4-64 studies, cells were incubated with 16 μM N-(3-triethylammoniumpropyl)-4-(p-diethylaminophenylhexatrien yl) pyridinium dibromide (FM 4-64) (Molecular Probes) at 30°C for 15 min then washed in YPD and incubated for an additional 15 or 45 min at 30°C. Images were collected on a fluorescence microscope equipped with a rhodamine filter and acquired using a CCD camera (model 4995; COHU), an integrator box (model 440A; Colorado Video, Inc.), and an LG-3 Frame Grabber (Scion Corp.). The software used was NIH Image 1.55 and Adobe Photoshop 4.0.

For electron microscopy, cells were grown in YPD at 30°C to an A_{600} of approximately 0.4. Fifty A_{600} units of cells were harvested by centrifugation, fixed, and processed as described previously (Cowles et al., 1994).

Acknowledgments

We thank S. Nothwehr and J. Thorner for providing *STE13* reagents; R. Doolittle for assistance with phylogenetic analysis; A. Abanes-DeMello and J. Sonnenburg for halo enhancement screen contributions; M. Babst and M. Seaman for sizing column fractions; T. Darsow for affinity purified anti-Vam3p antiserum; R. Aroian, J. Pogliano, and K. Pogliano for assistance with Delta Vision software; J. M. McCaffery for EM analysis (Core B of CA 58689); W. B. Snyder for provision of the M. Rose library; M. S. Robinson for sharing unpublished results; and members of the Emr lab for helpful discussion. C. R. C. is a member of the Biomedical Sciences Graduate program and a Lucille P. Markey Charitable Trust predoctoral fellow. G. O. is an Associate of the Howard Hughes Medical Institute. This work was supported by grants from the NIH (GM32703 and CA58689 to S. D. E.; GM39040 to G. S. P.). S. D. E. is an Investigator of the Howard Hughes Medical Institute.

Received July 21, 1997; revised August 26, 1997.

References

Babst, M., Sato, T.K., Banta, L.M., and Emr, S.D. (1997). Endosomal transport function in yeast requires a novel AAA-type ATPase, Vps4p. EMBO J. *16*, 1820–1831.

Bankaitis, V.A., Johnson, L.M., and Emr, S.D. (1986). Isolation of yeast mutants defective in protein targeting to the vacuole. Proc. Natl. Acad. Sci. USA *83*, 9075–9079.

Baudin, A., Ozier-Kalogeropoulos, O., Denouel, A., Lacroute, F., and Cullin, C. (1993). A simple and efficient method for direct gene deletion in Saccharomyces cerevisiae. Nucl. Acids Res. *21*, 3329–3330.

Burkhardt, J.K., Wiebel, F.A., Hester, S., and Argon, Y. (1993). The giant organelles in beige and Chediak-Higashi fibroblasts are derived from late endosomes and mature lysosomes. J. Exp. Med. *178*, 1845–1856.

Chan, R.K., and Otte, C.A. (1982). Isolation and genetic analysis of Saccharomyces cerevisiae mutants supersensitive to G_1 arrest by **a**-factor and α-factor pheromones. Mol. Cell. Biol. *2*, 11–20.

Cowles, C.R., Emr, S.D., and Horazdovsky, B.F. (1994). Mutations in the *VPS45* gene, a *SEC1* homolog, result in vacuolar protein sorting defects and accumulation of membrane vesicles. J. Cell Sci. *107*, 3449–3459.

Cowles, C.R., Snyder, W.B., Burd, C.G., and Emr, S.D. (1997). Novel Golgi to vacuole delivery pathway in yeast: identification of a sorting determinant and required transport component. EMBO J. *16*, 2769–2782.

Darsow, T., Rieder, S.E., and Emr, S.D. (1997). A multispecificity syntaxin homolog, Vam3p, essential for autophagic and biosynthetic protein transport to the vacuole. J. Cell Biol. *138*, 517–529.

Dell'Angelica, E.C., Ohno, H., Eng Ooi, C., Rabinovich, E., Roche, K.W., and Bonifacino, J.S. (1997). AP-3: an adaptor-like protein complex with ubiquitous expression. EMBO J. *16*, 917–928.

Feng, D., and Doolittle, R.F. (1996). Progressive alignment of amino acid sequences and construction of phylogenetic trees from them. Meth. Enzymol. *266*, 368–382.

Fuller, R.S., Sterne, R.E., and Thorner, J. (1988). Enzymes required for yeast prohormone processing. Annu. Rev. Physiol. *50*, 345–362.

Heilker, R., Manning-Krieg, U., Zuber, J.-F., and Spiess, M. (1996). In vitro binding of clathrin adaptors to sorting signals correlates with endocytosis and basolateral sorting. EMBO J. *15*, 2893–2899.

Herman, P.K., Stack, J.H., and Emr, S.D. (1991). A genetic and structural analysis of the yeast Vps15 protein kinase - evidence for a direct role of Vps15p in vacuolar protein delivery. EMBO J. *10*, 4049–4060.

Horazdovsky, B.F., and Emr, S.D. (1993). The *VPS16* gene product associates with a sedimentable protein complex and is essential for vacuolar protein sorting in yeast. J. Biol. Chem. *268*, 4953–4962.

Horazdovsky, B.F., Cowles, C.R., Mustol, P., Holmes, M., and Emr, S.D. (1996). A novel RING-finger protein, Vps8p, functionally interacts with the small GTPase, Vps21p, to facilitate soluble vacuolar protein localization. J. Biol. Chem. *271*, 33607–33615.

Julius, D., Blair, L., Brake, A., Sprague, G., and Thorner, J. (1983). Yeast α factor is processed from a larger precursor polypeptide: the essential role of a membrane-bound dipeptidyl aminopeptidase. Cell *32*, 839–852.

Letourneur, F., and Klausner, R.D. (1992). A novel di-leucine motif and a tyrosine-based motif independently mediate lysosomal targeting and endocytosis of CD3 chains. Cell *69*, 1143–1157.

Marcusson, E.G., Horazdovsky, B.F., Cereghino, J.L., Gharakhanian, E., and Emr, S.D. (1994). The sorting receptor for yeast vacuolar carboxypeptidase Y is encoded by the *VPS10* gene. Cell *77*, 579–586.

Marks, M.S., Ohno, H., Kirchhausen, T., and Bonifacino, J.S. (1997). Protein sorting by tyrosine-based signals. Trends Cell Biol. *7*, 124–128.

Newman, L.S., Mckeever, M.O., Okano, H.J., and Darnell, R.B. (1995). beta-NAP, a cerebellar degeneration antigen, is a neuron-specific vesicle coat protein. Cell *82*, 773–783.

Nothwehr, S.F., Roberts, C.J., and Stevens, T.H. (1993). Membrane protein retention in the yeast golgi apparatus - dipeptidyl aminopeptidase-A is retained by a cytoplasmic signal containing aromatic residues. J. Cell Biol. *121*, 1197–1209.

Panek, H.R., Stepp, J.D., Engle, H.M., Marks, K.M., Tan, P.K., Lemmon, S.K., and Robinson, L.C. (1997). Suppressors of YCK-encoded yeast casein kinase 1 deficiency define the four subunits of a novel clathrin AP-like complex. EMBO J. *16*, 4194–4204.

Phan, H.L., Finlay, J.A., Chu, D.S., Tan, P.K., Kirchhausen, T., and Payne, G.S. (1994). The Saccharomyces cerevisiae *APS1* gene encodes a homolog of the small subunit of the mammalian clathrin AP-1 complex - evidence for functional interaction with clathrin at the Golgi complex. EMBO J. *13*, 1706–1717.

Rad, M.R., Phan, H.L., Kirchrath, L., Tan, P.K., Kirchhausen, T., Hollenberg, C.P., and Payne, G.S. (1995). Saccharomyces cerevisiae Apl2p, a homologue of the mammalian clathrin AP beta subunit, plays a role in clathrin-dependent Golgi functions. J. Cell Sci. *108*, 1605–1615.

Radisky, D.C., Snyder, W.B., Emr, S.D., and Kaplan, J. (1997). Characterization of *VPS41*, a gene required for vacuolar trafficking and high-affinity iron transport in yeast. Proc. Natl Acad. Sci. USA *94*, 5662–5666.

Raymond, C.K., Howald-Stevendon, I., Vater, C.A., and Stevens, T.H. (1992). Morphological classification of the yeast vacuolar protein sorting mutants: evidence for a prevacuolar compartment in class E *vps* mutants. Mol. Biol. Cell *3*, 1389–1402.

Robinson, M.S. (1994). The role of clathrin, adaptors, and dynamin in endocytosis. Curr. Opin. Cell Biol. *6*, 538–544.

Robinson, M.S. (1997). Coats and vesicle budding. Trends Cell Biol. *7*, 99–102.

Robinson, J.S., Klionsky, D.J., Banta, L.M., and Emr, S.D. (1988). Protein sorting in Saccharomyces cerevisiae: isolation of mutants

defective in the delivery and processing of multiple vacuolar hydrolases. Mol. Cell. Biol. *8*, 4936–4948.

Robinson, J.S., Graham, T.R., and Emr, S.D. (1991). A putative zinc finger protein, Saccharomyces cerevisiae Vps18p, affects late Golgi functions required for vacuolar protein sorting and efficient α-factor prohormone maturation. Mol. Cell. Biol. *12*, 5813–5824.

Rothman, J.H., Howald, I., and Stevens, T.H. (1989). Characterization of genes required for protein sorting and vacuolar function in the yeast Saccharomyces cerevisiae. EMBO J. *8*, 2057–2065.

Sanger, F., Nicklen, F., and Coulson, A.R. (1977). DNA sequencing with chain-terminating inhibitors. Proc. Natl. Acad. Sci. USA *74*, 5463–5467.

Schekman, R., and Orci, L. (1996). Coat proteins and vesicle budding. Science *271*, 1526–1533.

Seeger, M., and Payne, G.S. (1992). A role for clathrin in the sorting of vacuolar proteins in the Golgi complex of yeast. EMBO J. *11*, 2811–2818.

Sherman, F., Fink, G.R., and Lawrence, L.W. (1979). Methods in Yeast Genetics: A Laboratory Manual. (Cold Spring Harbor, NY: Cold Spring Harbor Laboratory).

Sikorski, R.S., and Hieter, P. (1989). A system of shuttle vectors and yeast host strains designed for efficient manipulation of DNA in Saccharomyces cerevisiae. Genetics *122*, 19–27.

Simpson, F., Bright, N.A., West, M.A., Newman, L.S., Darnell, R.B., and Robinson, M.S. (1996). A novel adaptor-related protein complex. J. Cell Biol. *133*, 749–760.

Simpson, F., Peden, A.A., Christopoulou, L., and Robinson, M.S. (1997). Characterization of the adaptor-related protein complex, AP-3. J. Cell Biol. *137*, 835–845.

Spormann, D.O., Heim, J., and Wolf, D.H. (1992). Biogenesis of the yeast vacuole (lysosome) - the precursor forms of the soluble hydrolase carboxypeptidase yscS are associated with the vacuolar membrane. J. Biol. Chem. *267*, 8021–8029.

Sprague, G., Jr., Rine, J., and Herskowitz, I. (1981). Control of yeast cell type by the mating type locus. II. Genetic interactions between *MAT*α and unlinked α-specific *STE* genes. J. Mol. Biol. *153*, 323–335.

Stack, J.H., Dewald, D.B., Takegawa, K., and Emr, S.D. (1995). Vesicle-mediated protein transport: regulatory interactions between the Vps15 protein kinase and the Vps34 PtdIns 3-kinase essential for protein sorting to the vacuole in yeast. J. Cell Biol. *129*, 321–334.

Stepp, J.D., Pellicena-Palle, A., Hamilton, S., Kirchhausen, T., and Lemmon, S.K. (1995). A late Golgi sorting function for Saccharomyces cerevisiae Apm1p, but not for Apm2p, a second yeast clathrin AP medium chain-related protein. Mol. Biol. Cell *6*, 41–58.

Vida, T.A., and Emr, S.D. (1995). A new vital stain for visualizing vacuolar membrane dynamics and endocytosis in yeast. J. Cell Biol. *128*, 779–792.

Vida, T.A., Huyer, G., and Emr, S.D. (1993). Yeast vacuolar proenzymes are sorted in the late Golgi complex and transported to the vacuole via a prevacuolar endosome-like compartment. J. Cell Biol. *121*, 1245–1256.

Wada, Y., Nakamaru, N., Ohsumi, Y., and Hirata, A. (1997). Vam3p, a new member of syntaxin related protein, is required for vacuolar assembly in the yeast Saccharomyces cerevisiae. J. Cell Sci. *110*, 1299–1306.

Webb, G.C., Zhang, J., Garlow, S.J., Wesp, A., Riezman, H., and Jones, E.W. (1997). Pep7p provides a novel protein that functions in vesicle-mediated transport between the yeast Golgi and endosome. Mol. Biol. Cell *8*, 871–895.

Wilcox, C.A., Redding, K., Wright, R., and Fuller, R.S. (1992). Mutation of a tyrosine localization signal in the cytosolic tail of yeast Kex2 protease disrupts golgi retention and results in default transport to the vacuole. Mol. Biol. Cell *3*, 1353–1371.

Yon, J., and Fried, M. (1989). Precise gene fusion by PCR. Nucl. Acids Res. *17*, 4895.